| Title | Outage Probabilities of Orthogonal Multiple-Access Relaying Techniques with Imperfect Source-Relay Links |
|---|---|
| Author(s) | Lu, Pen-Shun; Zhou, Xiaobo; Matsumoto, Tad |
| Citation | IEEE Transactions on Wireless Communications |
| Issue Date | 2014-12-18 |
| Type | Journal Article |
| Text version | author |
| URL | http://hdl.handle.net/10119/12330 |
| Rights | This is the author's version of the work. Copyright (C) 2014 IEEE. IEEE Transactions on Wireless Communications, 2014, DOI:10.1109/TWC.2014.2384046. Personal use of this material is permitted. Permission from IEEE must be obtained for all other uses, in any current or future media, including reprinting/republishing this material for advertising or promotional purposes, creating new collective works, for resale or redistribution to servers or lists, or reuse of any copyrighted component of this work in other works. |
| Description | |

# Outage Probabilities of Orthogonal Multiple-Access Relaying Techniques with Imperfect Source-Relay Links

Pen-Shun Lu, *Student Member, IEEE,* Xiaobo Zhou, *Member, IEEE,* and Tad Matsumoto, *Fellow, IEEE*

*Abstract*—An outage probability that is independent of sig-naling schemes is theoretically derived in this paper for an orthogonal multiple-access relay channel (MARC) system, where the estimates of the information sequences sent from source nodes, regardless of whether or not they are correctly decoded at the relay, are exclusive-OR (XOR)-network-coded and forwarded by the relay to the destination. The MARC system described above is referred to as estimates-exploiting MARC (e-MARC) in this paper for convenience. Following the probability derivation of e-MARC, comparisons are then made with the outage probability of the orthogonal MARC with the Select Decode-and-Forward relaying strategy (MARC-SDF). It is found through simulations that when one of the source nodes is far away from both the relay and the destination, the e-MARC system is superior to MARC-SDF in terms of outage performance. We further numerically calculate the outage probabilities for two special cases, and compare them with the probability of e-MARC. Furthermore, the impact of the source correlation on the outage probability of the e-MARC system is also investigated.

*Index Terms*—multiple access relay channel, outage probabil-ity, decode-and-forward, Slepian-Wolf theorem, source-channel separation theorem.

## I. INTRODUCTION

COOPERATIVE wireless networks have attracted a lot of attention of the wireless communication research community recently, since they provide a lot of design flexi-bility in the form of, e.g., coverage extension, and a variety of methodologies for multiple users quality-of-service (QoS) management. One of the cooperative wireless networks is multiple access relay [1], which consists of multiple source nodes, one relay and one common destination. The role of the relay is to assist the source nodes to improve the probability of successful transmission to the destination.

In multiple access relay channel (MARC) systems, decoded-and-forward (DF) is one of the most popular relaying strate-gies, and many DF-based excellent joint network-and-channel coding (JNCC) techniques for MARC systems have been

Pen-Shun Lu and Tad Matsumoto are with Centre for Wireless Com-munications, P.O. Box 4500, 90014 University of Oulu, Finland, and with School of Information Science, Japan Advanced Institute of Science and Tech-nology, 1-1 Asahidai, Nomi, Ishikawa, 923-1292 Japan (e-mail: {penshun, tadashi.matsumoto}@ee.oulu.fi).

Xiaobo Zhou is with Centre for Wireless Communications, P.O. Box 4500, 90014 University of Oulu, Finland (e-mail: {zhouxiaobo07}@gmail.com).

developed [2]–[7]. Most of the DF strategies used at the relay discard the information sequence estimates containing errors at the relay. This is because forwarding the erroneous estimates results in error propagation in the decoding process at the destination. As mentioned in [8], [9], performance and diversity gain are dramatically degraded due to the error propagation.

However, in practice, the source nodes are not geograph-ically always close enough to the relay, and the average received signal-to-noise power ratio (SNR) is determined by the pathloss. Furthermore, the signal/signals received by the nodes may suffer from deep fade, depending on their locations. Error occurring in the source-relay links may well be elim-inated by using powerful, capacity-achieving channel codes in the signaling scheme. Nevertheless, in many cases, the use of the powerful, close-capacity achieving codes per-link does not always provide reasonable solutions. This is because large latency is induced due to the iterative decoding process; moreover, the battery and memory resources of the relay may be limited to perform complicated decoding algorithms.

Quite recently, several excellent techniques have been pro-posed to exploit the erroneous estimates obtained at the relay [9]–[20]. In [16], the erroneous estimates of the infor-mation sent from the source nodes are, instead of discarding them, exclusive-OR (XOR)-network-coded at the relay, and forwarded to the destination to help reconstruct the informa-tion sequences; this MARC system is referred to as estimates-exploiting MARC (e-MARC) in this paper. The erroneous estimates in [16] are exploited in the decoding process at the destination by utilizing the knowledge of the bit-flipping probability $p_{nc}$ between the two sequences: one is the network-coded sequence sent from the relay, and the other is its corresponding XOR-ed information sequence. The bit-flipping probability $p_{nc}$ is referred to as *network correlation* in this paper.

Unlike techniques for the outage probability analysis [8], [21]–[24] for the cases where the relay stops forwarding if the estimates are found to contain error(s) at the relay, this paper analyzes the outage probability of e-MARC where erroneous estimates at the relay are further forwarded. The goal of this paper is twofold: (i) to re-formulate the e-MARC system according to the framework of the Slepian-Wolf theorem [25] for correlated source coding with a helper and analyze the e-MARC system's admissible rate region according to the re-formulation, and (ii) to derive the outage probability of the e-MARC system where all five links in the system (two
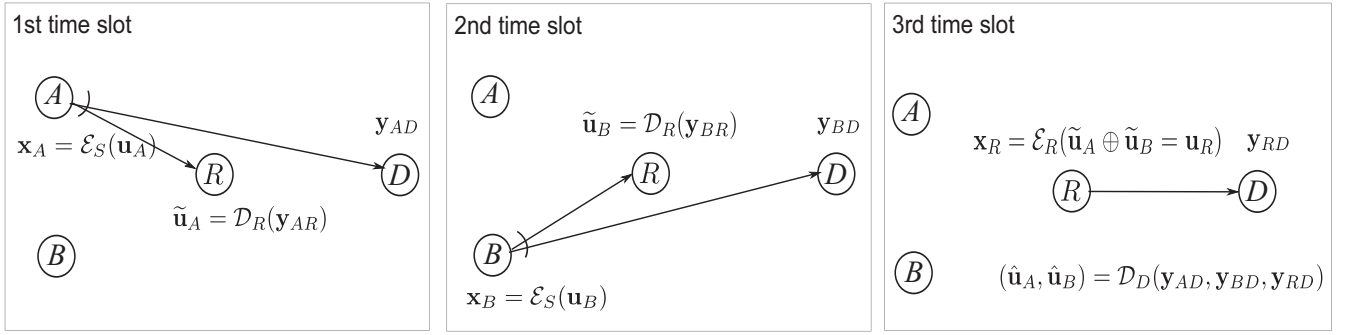
Fig. 1.   Orthogonal e-MARC system model, where there are three time slots in a transmission cycle.

source-destination links, two source-relay links and one relay-destination link) are suffering from statistically independent block Rayleigh fading.

The theoretical analyses are based on the techniques presented in [26], [27]. However, in [26], the source-relay link(s) is assumed to be static, while in [27], they are assumed to be perfect, of which assumptions are not practical in real scenarios. In this paper, fading is taken into account in the source-relay link, and thus the source-relay link's error probability becomes a random variable, which makes the analysis for the admissible rate region to be challenging. Furthermore, to be able to compare with the theoretical outage performances of other relaying strategies applied in MARC, a theoretical limit of the source-relay link's error probability is found by utilizing the rate-distortion and inverse capacity functions in this paper. Then, it is shown that the outage probability of the e-MARC system, independent of signaling schemes, can be theoretically derived by a fivefold-integral over the admissible rate region with respect to the probability density functions (pdfs) of the five links' instantaneous SNRs.

The e-MARC system is then compared with network-coding-based orthogonal MARC systems (MARC-NC) [8] and orthogonal MARC with the select decode-and-forward relaying strategy (MARC-SDF) [24] in terms of the outage performance. It is observed through simulations that e-MARC is superior to MARC-NC. Furthermore, in Asymmetric scenario where one of the source nodes is far away from both the relay and the destination, e-MARC achieves better performance than MARC-SDF.

In addition, the process for deriving the probability is then applied to the following two special cases.

1) Source-relay links are assumed to be binary-symmetric channels (BSCs), and

2) The e-MARC system with practical signaling schemes presented in [16], where the relay only *extracts* (EX) the estimates output from differential detector (DD). The e-MARC system where the relay applies the detection strategy mentioned above is referred to as DDEX e-MARC system in this paper.

The fivefold-integral needed to obtain the outage probability can be reduced to simpler expressions, corresponding to their error probabilities of source-relay links. Numerical results show that theoretical outage probabilities with the DDEX e-MARC system are roughly 3.5 and 4.5 dB away from the probabilities of the e-MARC system independent of

signaling schemes in Symmetric and Asymmetric scenarios, respectively. This performance loss is due to the reason that we aim to reduce the computational complexity.

Finally, this paper investigates the impact of the correlation between the two source nodes on the outage probability of the e-MARC system. It is found that for the case two source nodes are highly correlated, the outage performance can still be improved by exploiting the *source correlation* even if only one of the source-destination links is reliable.

The rest of this paper is organized as follows: Section II introduces the system model of the e-MARC system assumed in this paper. The outage probability for e-MARC systems is theoretically derived in Section III. Numerical results of the outage probabilities for the universal case and two special cases are presented in Section IV. Furthermore, the results of simulations are presented to evaluate the performance of the scheme presented in [16] in terms of frame error rate (FER) in Section IV. Also, the theoretical outage probabilities of MARC-NC and that of MARC-SDF are included in Section IV for comparisons. The impact of the source correlation and network correlation on the outage probability is discussed in Section V. Finally, Section VI concludes the paper.

## II. SYSTEM MODEL

Fig. 1 illustrates a basic model of the orthogonal e-MARC system assumed in this paper, where there are two source nodes $A$ and $B$, one common relay $R$, and one common destination $D$. The $K$-bit length independent identically distributed (i.i.d.) binary information sequences generated from nodes $A$ and $B$ are denoted as $\mathbf{u}_A = \{u_A(k)\}_{k=1}^K$ and $\mathbf{u}_B = \{u_B(k)\}_{k=1}^K$, respectively. The signaling scheme used at the source node is denoted as $\mathcal{E}_S(\cdot)$, which consists of a serial concatenation of channel encoding and modulation. There are three time slots in one transmission cycle. In the first two time slots, nodes $A$ and $B$ respectively broadcast their coded sequences $\mathbf{x}_A = \mathcal{E}_S(\mathbf{u}_A) = \{x_A(m)\}_{m=1}^M$ and $\mathbf{x}_B = \mathcal{E}_S(\mathbf{u}_B) = \{x_B(m)\}_{m=1}^M$ to the relay $R$ and destination $D$, and their corresponding received signals obtained at $R$ and $D$ are respectively written as

$$\mathbf{y}_{iR} = h_{iR} \cdot \mathbf{x}_i + \mathbf{n}_{iR}$$
$$\mathbf{y}_{iD} = h_{iD} \cdot \mathbf{x}_i + \mathbf{n}_{iD}, \qquad i \in \{A, B\} \qquad (1)$$

where $h_{iR}$ and $h_{iD}$ indicate the channel coefficients of $iR$ and $iD$ links with the source node $i$, respectively. $\mathbf{n}_{iR}$ and

TABLE I
NOTATIONS.

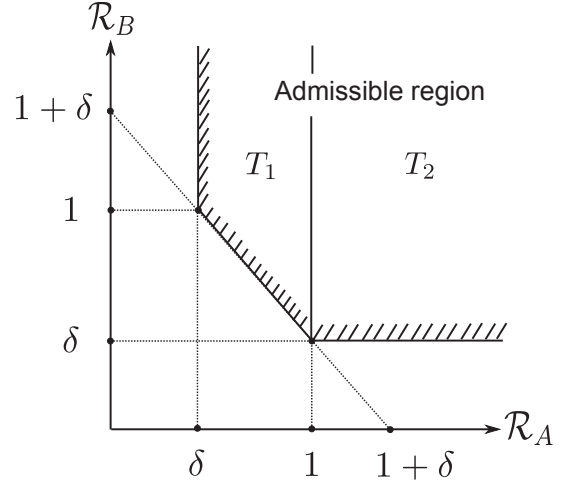| | |
|---|---|
| $i$ | Source node, $i \in \{A, B\}$ |
| $R$ | Relay |
| $D$ | Destination |
| $\mathbf{u}_i$ | Information sequence of $i$ |
| $\widetilde{\mathbf{u}}_i$ | Estimates of $\mathbf{u}_i$ received at $R$ |
| $\hat{\mathbf{u}}_i$ | Estimates of $\mathbf{u}_i$ received at $D$ |
| $\mathbf{x}_i$ | Coded sequences of node $i$ |
| $\mathbf{y}_{iR}$ | Received signals at $R$ sent from $i$ |
| $\mathbf{y}_{iD}$ | Received signals at $D$ sent from $i$ |
| $\mathbf{y}_{RD}$ | Received signals at $D$ sent from $R$ |
| $p_i$ | Error probability/ rate of $iR$ link |
| $p_R$ | Error probability/ rate of $RD$ link |
| $\hat{p}_i$ | Theoretical limit of $p_i$ |
| $\hat{p}_R$ | Theoretical limit of $p_R$ |
| $\tilde{p}_i$ | Non zero value of $\hat{p}_i$ |
| $\tilde{p}_R$ | Non zero value of $\hat{p}_R$ |
| $\gamma_{iR}$ | Instantaneous SNR of $iR$ link |
| $\gamma_{iD}$ | Instantaneous SNR of $iD$ link |
| $\gamma_{RD}$ | Instantaneous SNR of $RD$ link |
| $\gamma_i^*$ | $p_i = 0$ if $\gamma_{iR} > \gamma_i^*$ |
| $\gamma_R^*$ | $p_R = 0$ if $\gamma_{RD} > \gamma_R^*$ |
| $\mathcal{E}_S$ | Signaling scheme at $i$ |
| $\mathcal{E}_R$ | Signaling scheme at $R$ |
| $\mathcal{R}_i$ | Source coding rate at $i$ |
| $\mathcal{R}_R$ | Source coding rate at $R$ |
| $\mathcal{R}_{ci}$ | Spectrum efficiency of $\mathcal{E}_S$ |
| $\mathcal{R}_{cR}$ | Spectrum efficiency of $\mathcal{E}_R$ |
| $H_b(\cdot)$ | Binary entropy function |
| $*$ | convolution, $\alpha * \beta = \alpha(1-\beta) + \beta(1-\alpha)$ |
| $\delta$ | $H_b(p_A * p_B * p_R)$ |
| $\hat{\delta}$ | Theoretical limit of $\delta$ |
| $\ddot{\delta}$ | $\delta$ with constant $p_i$ |
| $p_s$ | Source correlation |
| $p_{nc}$ | Network correlation; $p_{nc} = p_A * p_B$ |



Fig. 2. Admissible rate region of the rate pair $(\mathcal{R}_A, \mathcal{R}_B)$ given $\mathcal{R}_R \geq I(\mathbf{u}_R; \hat{\mathbf{u}}_R)$ for lossless compression, where $\delta = H_b(p_A * p_B * p_R)$.

is denoted as $\hat{\mathbf{u}}_R$, and the error rate of the $RD$ link is $p_R = \mathfrak{B}(\mathbf{u}_R, \hat{\mathbf{u}}_R)$. Finally, to obtain the estimates $\hat{\mathbf{u}}_A$ and $\hat{\mathbf{u}}_B$ of the information sequences $\mathbf{u}_A$ and $\mathbf{u}_B$, respectively, at the destination, decoding of JNCC is performed on the received signal vectors $\mathbf{y}_{AD}$ and $\mathbf{y}_{BD}$ with the help of the signal vector $\mathbf{y}_{RD}$.

All the links in this paper are assumed to suffer from block Rayleigh fading, with which $h_{iR}$, $h_{iD}$ and $h_{RD}$ are assumed to be constant over one coded sequence but vary independently transmission-by-transmission and link-by-link. Without loss of generality, we assume that $E[|h_{iR}|^2] = E[|h_{iD}|^2] = E[|h_{RD}|^2] = 1$. The error rates $p_i$ and $p_R$, thus, vary in each transmission cycle. The instantaneous SNRs $\gamma_{iR}, \gamma_{iD}$ and $\gamma_{RD}$ of the links are then given by

$$\gamma_{iR} = |h_{iR}|^2 \cdot \Gamma_{iR}$$
$$\gamma_{iD} = |h_{iD}|^2 \cdot \Gamma_{iD}$$
$$\gamma_{RD} = |h_{RD}|^2 \cdot \Gamma_{RD} \quad (5)$$

where $\Gamma_{iR}$, $\Gamma_{iD}$ and $\Gamma_{RD}$ represent the average SNRs of the intra, direct and $RD$ links, respectively.

## III. DERIVATION FOR OUTAGE PROBABILITY OF E-MARC

### A. Outage event for each transmission cycle

The outage probability of the e-MARC system is derived in this section. The e-MARC system model shown in Fig. 1 can be viewed as a system having two source nodes $A$ and $B$, and one helper $R$. Letting $\mathcal{R}_A$ and $\mathcal{R}_B$ be the source coding rate of $A$ and $B$, respectively. To investigate the admissible rate region for the two independent source nodes with one helper, we thus invoke the theorem [28, Theorem 10.4.], according to which the information sequences $\mathbf{u}_A$ and $\mathbf{u}_B$ can be successfully recovered at the destination if

$\mathbf{n}_{iD}$ indicate the vectors of independent zero-mean complex additive white Gaussian noise (AWGN) of the $iR$ and $iD$ links, respectively, with variance $\sigma_{iR}^2 = \sigma_{iD}^2 = \sigma^2$ per dimension. The $iR$ and $iD$ links are also referred to as the intra and direct links, respectively, in this paper.

The receiver applied at the relay $R$ is denoted as $\mathcal{D}_R(\cdot)$, composed of signal detection and decoding, which corresponds to the inverse structure of $\mathcal{E}_S(\cdot)$. The estimates $\widetilde{\mathbf{u}}_i = \mathcal{D}_R(\mathbf{y}_{iR})$ of $\mathbf{u}_i$ obtained at $R$ may contain errors due to the variation of the $iR$ link. The error rate of the $iR$ link is represented by

$$p_i = \mathfrak{B}(\mathbf{u}_i, \widetilde{\mathbf{u}}_i) = \frac{\sum_{k=1}^{K} |u_i(k) - \widetilde{u}_i(k)|}{K}, \quad i \in \{A, B\}. \quad (2)$$

In the e-MARC system model, the estimates $\widetilde{\mathbf{u}}_A$ and $\widetilde{\mathbf{u}}_B$, are always joint network-channel coded at $R$ regardless of whether they are correct or not, as

$$\mathbf{x}_R = \mathcal{E}_R(\mathbf{u}_R) = \mathcal{E}_R(\widetilde{\mathbf{u}}_A \oplus \widetilde{\mathbf{u}}_B), \quad (3)$$

where the notation $\oplus$ denotes a binary exclusive-OR (XOR) operation and $\mathcal{E}_R(\cdot)$ represents the signaling scheme applied at $R$, including channel encoding and modulation. The destination $D$ obtains the signal vector $\mathbf{y}_{RD}$ of $\mathbf{x}_R$ sent via the relay-destination ($RD$) link as

$$\mathbf{y}_{RD} = h_{RD} \cdot \mathbf{x}_R + \mathbf{n}_{RD}, \quad (4)$$

where $h_{RD}$ and $\mathbf{n}_{RD}$ indicate the channel coefficient and AWGN vector of the $RD$ link with variance $\sigma_{RD}^2 = \sigma^2$, respectively. The estimates of $\mathbf{u}_R$ obtained at the destination

$$\mathcal{R}_A \geq H(\mathbf{u}_A|\mathbf{u}_B, \hat{\mathbf{u}}_R),$$
$$\mathcal{R}_B \geq H(\mathbf{u}_B|\mathbf{u}_A, \hat{\mathbf{u}}_R),$$
$$\mathcal{R}_A + \mathcal{R}_B \geq H(\mathbf{u}_A, \mathbf{u}_B|\hat{\mathbf{u}}_R),$$
$$\mathcal{R}_R \geq I(\mathbf{u}_R; \hat{\mathbf{u}}_R), \tag{6}$$

where $\mathcal{R}_R$ represents the source coding rate at $R$, and the coded side information provided by the relay $R$ (helper) helps reduce the rate $\mathcal{R}_A$ and $\mathcal{R}_B$. Then, by using the chain rule, (6) can be re-formulated (see Appendix A) as follows

$$\mathcal{R}_A \geq \delta, \tag{7a}$$
$$\mathcal{R}_B \geq \delta, \tag{7b}$$
$$\mathcal{R}_A + \mathcal{R}_B \geq \delta + 1, \tag{7c}$$
$$\mathcal{R}_R \geq 1 - H_b(p_R), \tag{7d}$$

where

$$\delta = H_b(p_A * p_B * p_R). \tag{8}$$

The operation $\alpha * \beta$ is defined as $\alpha(1 - \beta) + \beta(1 - \alpha)$, and $H_b(\cdot)$ denotes the binary entropy function [29]. To simplify the derivation, we first assume that the inequality (7d) is satisfied. With a given $\mathcal{R}_R$, the admissible rate region of $(\mathcal{R}_A, \mathcal{R}_B)$ for each transmission cycle is obtained, as shown in Fig. 2.

For a transmission cycle, the outage event is defined as: one or both of the information sequences $\mathbf{u}_A$ and $\mathbf{u}_B$ cannot be successfully recovered at the destination. Therefore, given a value of $\mathcal{R}_R$, the outage event happens when the pair $(\mathcal{R}_A, \mathcal{R}_B)$ falls outside the admissible rate region. As shown in Fig. 2, the entire admissible rate region can be divided into two parts $T_1$ and $T_2$. $\varepsilon_1$ and $\varepsilon_2$ denote the events that the rate pair $(\mathcal{R}_A, \mathcal{R}_B)$ falls into $T_1$ and $T_2$, respectively, as

$$\varepsilon_1 = \{(\mathcal{R}_A, \mathcal{R}_B) \in T_1\}$$
$$= \{\delta \leq \mathcal{R}_A \leq 1\} \wedge \{\mathcal{R}_A + \mathcal{R}_B \geq \delta + 1\},$$
$$\varepsilon_2 = \{(\mathcal{R}_A, \mathcal{R}_B) \in T_2\} = \{\mathcal{R}_A \geq 1\} \wedge \{\mathcal{R}_B \geq \delta\}. \tag{9}$$

where the symbols '$\vee$' and '$\wedge$' denote as the logical '*or*' and '*and*' operators, respectively. Therefore, with the assumption that (7d) is satisfied, the outage event of the e-MARC system for each transmission cycle is obtained, as

$$\text{OUT} = \overline{\{\varepsilon_1 \vee \varepsilon_2\}}. \tag{10}$$

where the $\overline{\{\varepsilon_1 \vee \varepsilon_2\}}$ denotes the complement of event $\{\varepsilon_1 \vee \varepsilon_2\}$.

According to Shannon's source-channel separation theorem, the relationship between the instantaneous SNR $\gamma_{iD}$ and its corresponding source coding rate $\mathcal{R}_i$ is given by [30]

$$\mathcal{R}_i = \frac{C(\gamma_{iD})}{\mathcal{R}_{ci}} = f_i(\gamma_{iD}), \qquad i \in \{A, B\} \tag{11}$$

where it is assumed that a capacity-achieving channel code is used in $iD$ link. Here $\mathcal{R}_{ci}$ represents the spectrum efficiency of the signaling scheme $\mathcal{E}_S(\cdot)$, including the channel coding scheme and the modulation multiplicity, and $C(\alpha) = \log_2(1 +$

$\alpha)$. It should be emphasized that the optimality of source-channel separation holds for Rayleigh fading MARC systems where all the links are orthogonal [31], [32].

Since the function $f_i(\cdot)$ is one-to-one mapping, the events $\varepsilon_1$ and $\varepsilon_2$ can be, respectively, expressed as

$$\varepsilon_1 = \{f_A^{-1}(\delta) \leq \gamma_{AD} \leq f_A^{-1}(1)\} \wedge \{f_B^{-1}(\omega) \leq \gamma_{BD}\}$$
$$\varepsilon_2 = \{f_A^{-1}(1) \leq \gamma_{AD}\} \wedge \{f_B^{-1}(\delta) \leq \gamma_{BD}\}, \tag{12}$$

where

$$\omega = \delta + 1 - f_A(\gamma_{AD}). \tag{13}$$

### B. Theoretical limits of $p_A$ and $p_B$

The boundaries of the events $\varepsilon_1$ and $\varepsilon_2$ in (12) are involved with the $iR$ link error probability[1] $p_i$, and the value of the $p_i$ is a function of $\gamma_{iR}$. However, the relationship between $p_i$ and $\gamma_{iR}$ depends on the signaling schemes employed in the $iR$ link. Furthermore, it is quite common that $p_i$ cannot be explicitly expressed as a function of $\gamma_{iR}$, if specific channel coding or modulation schemes are used. Therefore, instead, we aim to derive a theoretical limit for the value of $p_i$, given a $\gamma_{iR}$ value in the following.

According to Shannon's lossy source-channel separation theorem [33], the information sequence $\mathbf{u}_i$ can be transmitted over the $iR$ link with a distortion level $\mathfrak{D}_i$ if

$$\mathcal{R}_i(\mathfrak{D}_i)\mathcal{R}_{ci} \leq C(\gamma_{iR}), \qquad i \in \{A, B\}. \tag{14}$$

With the Hamming distortion measure, the distortion $\mathfrak{D}_i$ is equivalent to the error probability $p_i$, and thus according to [29], the rate-distortion function $\mathcal{R}_i(\mathfrak{D}_i)$ is represented as

$$\mathcal{R}_i(\mathfrak{D}_i) = 1 - H_b(p_i). \tag{15}$$

By assuming that a capacity-achieving channel code is applied at the $iR$ link, the equality in (14) holds, yielding the theoretical limit $\hat{p}_i$ of $p_i$ for any given $\gamma_{iR}$, as

$$\hat{p}_i(\gamma_{iR}) = \begin{cases} H_b^{-1}(1 - f_i(\gamma_{iR})) = \tilde{p}_i(\gamma_{iR}), & 0 \leq \gamma_{iR} < \gamma_i^* \\ 0, & \gamma_{iR} \geq \gamma_i^* \end{cases} \tag{16}$$

where $H_b^{-1}(\cdot)$ denotes the inverse function of $H_b(\cdot)$, and $\gamma_i^*$ is a threshold value of the instantaneous SNR $\gamma_{iR}$ such that $f_i(\gamma_i^*) = 1$.

### C. Theoretical limit of $p_R$

In this subsection, the assumption that the inequality (7d) holds in (12) is eliminated, such that the variation of the rate $\mathcal{R}_R$ can be taken into account when deriving the outage probability in the next subsection. In the same way as deriving (11), the relationship between the instantaneous SNR $\gamma_{RD}$ and rate $\mathcal{R}_R$ can be expressed, as

---

[1]The length of information sequence $K$ is assumed to be infinite for deriving the fully theoretical outage probability.

$$\mathcal{R}_R = \frac{C(\gamma_{RD})}{\mathcal{R}_{cR}} = f_R(\gamma_{RD}) \geq 1 - H_b(p_R) \qquad (17)$$

where $\mathcal{R}_{cR}$ represents the spectrum efficiency of the signaling scheme $\mathcal{E}_R(\cdot)$. Considering the constraint imposed on $\mathcal{R}_R$ (i.e., $\mathcal{R}_R \geq 1 - H_b(p_R)$), it is found from (17) that, although the variation range of the rate $\mathcal{R}_R$ is $[0, \infty)$, $p_R$ is reduced to zero when the value of $\gamma_{RD}$ is larger than $f_R^{-1}(1)$. Therefore, by (17), the theoretical limit $\hat{p}_R$ of $p_R$ for any given instantaneous SNR value $\gamma_{RD}$, is

$$\hat{p}_R(\gamma_{RD}) = \begin{cases} H_b^{-1}(1 - f_R(\gamma_{RD})) = \tilde{p}_R(\gamma_{RD}), & 0 \leq \gamma_{RD} < \gamma_R^* \\ 0, & \gamma_{RD} \geq \gamma_R^*, \end{cases} \qquad (18)$$

where $\gamma_R^* = f_R^{-1}(1)$.

By replacing $p_i$ and $p_R$ with $\hat{p}_i(\gamma_{iR})$ and $\hat{p}_R(\gamma_{RD})$ in (12), respectively, the boundaries of events $\varepsilon_1$ and $\varepsilon_2$ in (12) are converted to the domains of instantaneous SNR, as

$$\varepsilon_1 = \{f_A^{-1}(\hat{\delta}) \leq \gamma_{AD} \leq f_A^{-1}(1)\} \wedge \{f_B^{-1}(\hat{\omega}) \leq \gamma_{BD}\}$$
$$\varepsilon_2 = \{f_A^{-1}(1) \leq \gamma_{AD}\} \wedge \{f_B^{-1}(\hat{\delta}) \leq \gamma_{BD}\}, \qquad (19)$$

where

$$\hat{\delta} = H_b(\hat{p}_A(\gamma_{AR}) * \hat{p}_B(\gamma_{BR}) * \hat{p}_R(\gamma_{RD}))$$
$$\hat{\omega} = \hat{\delta} + 1 - f_A(\gamma_{AD}). \qquad (20)$$

### D. Outage probability of e-MARC

Recall that in Section II all the links are assumed to be statistically independent and their corresponding instantaneous SNRs are Rayleigh distributed,[2] transmission-by-transmission and link-by-link. Hence, the probabilities of $\varepsilon_1$ and $\varepsilon_2$ are calculated, as

$$\Pr(\varepsilon_1) = \Pr\left(\{f_A^{-1}(\hat{\delta}) \leq \gamma_{AD} \leq f_A^{-1}(1)\} \wedge \{f_B^{-1}(\hat{\omega}) \leq \gamma_{BD}\}\right)$$
$$= \iiint_V \underbrace{\int_{f_A^{-1}(\hat{\delta})}^{f_A^{-1}(1)} p(\gamma_{AD}) d\gamma_{AD} \int_{f_B^{-1}(\hat{\omega})}^{\infty} p(\gamma_{BD}) d\gamma_{BD}}_{g_1} \cdot$$
$$p(\gamma_{AR}, \gamma_{BR}, \gamma_{RD}) d\gamma_{AR} d\gamma_{BR} d\gamma_{RD}$$
$$= \iiint_V \underbrace{\frac{1}{\Gamma_{AD}} \int_{f_A^{-1}(\hat{\delta})}^{f_A^{-1}(1)} \exp\left(\frac{-f_B^{-1}(\hat{\omega})}{\Gamma_{BD}} - \frac{\gamma_{AD}}{\Gamma_{AD}}\right) d\gamma_{AD}}_{g_1} \cdot$$
$$p(\gamma_{AR}) p(\gamma_{BR}) p(\gamma_{RD}) d\gamma_{AR} d\gamma_{BR} d\gamma_{RD}$$
$$= \Im[g_1; V] \qquad (21)$$

[2] $p(\gamma_q) = \frac{1}{\Gamma_q} \exp\left(-\frac{\gamma_q}{\Gamma_q}\right), \quad q \in \{AR, BR, AD, BD, RD\}$

and

$$\Pr(\varepsilon_2) = \Pr\left(\{f_A^{-1}(1) \leq \gamma_{AD}\} \wedge \{f_B^{-1}(\hat{\delta}) \leq \gamma_{BD}\}\right)$$
$$= \iiint_V \underbrace{\int_{f_A^{-1}(1)}^{\infty} p(\gamma_{AD}) d\gamma_{AD} \int_{f_B^{-1}(\hat{\delta})}^{\infty} p(\gamma_{BD}) d\gamma_{BD}}_{g_2} \cdot$$
$$p(\gamma_{AR}, \gamma_{BR}, \gamma_{RD}) d\gamma_{AR} d\gamma_{BR} d\gamma_{RD}$$
$$= \iiint_V \underbrace{\exp\left(\frac{-f_A^{-1}(1)}{\Gamma_{AD}} - \frac{f_B^{-1}(\hat{\delta})}{\Gamma_{BD}}\right)}_{g_2} \cdot$$
$$p(\gamma_{AR}) p(\gamma_{BR}) p(\gamma_{RD}) d\gamma_{AR} d\gamma_{BR} d\gamma_{RD}$$
$$= \Im[g_2; V], \qquad (22)$$

where the domain of the threefold integral is

$$V = \{(\gamma_{AR}, \gamma_{BR}, \gamma_{RD}) : \gamma_{AR} \in \mathbb{R}^+, \gamma_{BR} \in \mathbb{R}^+, \gamma_{RD} \in \mathbb{R}^+\},$$
$$\mathbb{R}^+ = [0, \infty). \qquad (23)$$

Finally, the outage probability of the e-MARC system can be obtained, as

$$P_{\text{out}} = 1 - (\Pr(\varepsilon_1) + \Pr(\varepsilon_2)). \qquad (24)$$

It may be difficult to calculate the integrals shown in (21) and (22) in closed form. Hence, the results of (21) and (22) in this paper are numerically obtained by using functions provided in [34]. Moreover, (21) and (22) can be respectively divided into eight sub-integrals according to different domains, which makes the numerical calculation of (21) and (22) tractable. The divisions of (21) and (22) are listed in Appendix B.

## IV. NUMERICAL RESULTS

### A. Outage probability of e-MARC

Fig. 3 shows the numerical results of the outage probability for the e-MARC system that are independent of signaling schemes, obtained by calculating from (24) with (21) and (22) shown in Section III, where $\Gamma_{AD} = \Gamma_{BD}$ and $\Gamma_{RD} = \Gamma_{AD} + 3$ dB is assumed. The values of $\mathcal{R}_{ci}$ and $\mathcal{R}_{cR}$ are set to $1/2$. The curve of the probability with perfect intra links is obtained from [27]. It is found that as the quality of intra links degrades, the gap increases between the probabilities with the perfect and with the imperfect intra links.

### B. Outage performance comparisons

To evaluate the impact of the utilization of the erroneous estimates received at the relay, we also compare the outage probability of the e-MARC system with the theoretical outage probabilities with MARC-NC [8] and MARC-SDF [24].

TABLE II
SETTINGS OF SYMMETRIC AND ASYMMETRIC SCENARIOS.

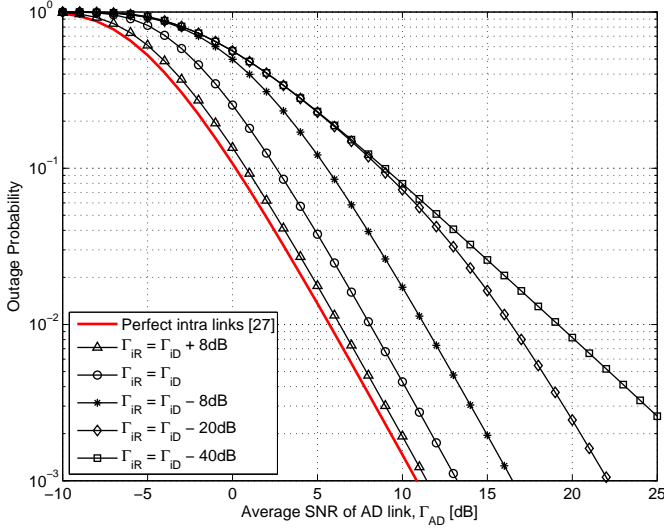| Scenario | $\Gamma_{AD}$ | $\Gamma_{BD}$ | $\Gamma_{AR}$ | $\Gamma_{BR}$ | $\Gamma_{RD}$ |
|---|---|---|---|---|---|
| Symmetric | $X$ | $X$ | $X+\Delta$ | $X+\Delta$ | $X+\Delta$ |
| Asymmetric | $X$ | $X$-$L$ | $X+\Delta$ | $X+\Delta$-$L$ | $X+\Delta$ |

Fig. 3. Outage probabilities of e-MARC that are independent of signaling schemes, where $\Gamma_{AD} = \Gamma_{BD}$ and $\Gamma_{RD} = \Gamma_{AD} + 3$ dB is assumed, and $\mathcal{R}_{ci} = \mathcal{R}_{cR} = 1/2$.
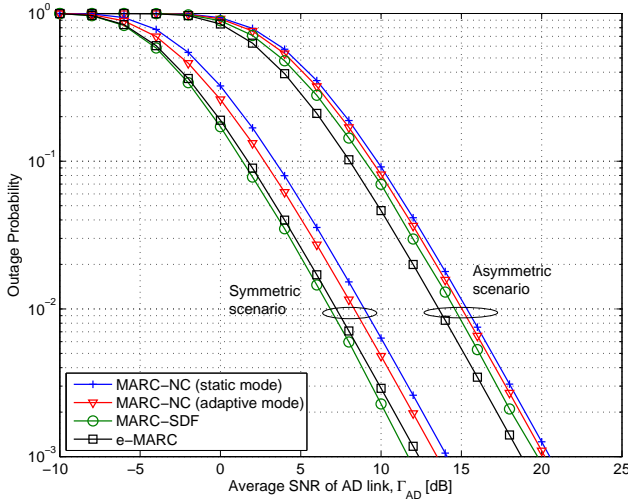


Fig. 4. Outage probabilities of e-MARC are in comparisons with those with MARC-NC [8], and with MARC-SDF [24]. $\mathcal{R}_{ci} = \mathcal{R}_{cR} = 1/2$.

Results of the outage probability analysis in Symmetric and Asymmetric scenarios are demonstrated in Fig. 4 for comparisons. The scenarios settings exemplifying the symmetric and asymmetric cases are summarized in Table II, where $X$ represents the average SNR of the $AD$ link in dB; $\Delta$ and $L$ denoting additional gain and loss due to the shorter and longer distance, respectively, and are set to 3 dB and 10 dB in this subsection.

The theoretical outage probabilities of MARC-NC, analyzed in a separate network-and-channel coding (SNCC) framework, were included in Fig. 4. The outage probabilities[3] in static and in adaptive mode are obtained by [8, eqs. (4)-(5)] and [8, eqs. (4),(8)-(9),(11)], respectively. It is found that the e-MARC system outperforms MARC-NC in terms of outage performance.

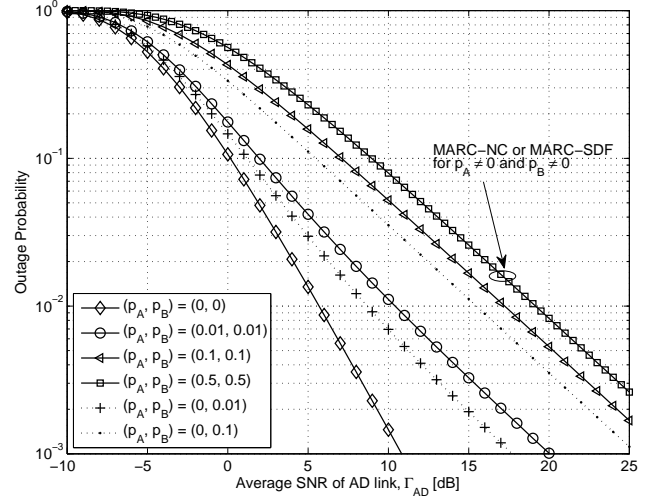In principle, as stated in [24], a header (i.e., flag) is



Fig. 5. Theoretical outage probabilities of e-MARC with static intra links, where $\Gamma_{AD} = \Gamma_{BD}$ and $\Gamma_{RD} = \Gamma_{AD} + 3$ dB. $\mathcal{R}_{ci} = \mathcal{R}_{cR} = 1/2$

used at the relay in MARC-SDF to identify the correctly decoded source nodes, and furthermore, the header has to be protected with a very powerful error correction code. On the other hand, the relay in e-MARC always performs network-coding and does not add header to the forwarded XOR-ed sequence. Therefore, it is not reasonable to make comparisons between MARC-SDF and e-MARC, because MARC-SDF and e-MARC belong to different categories of MARC (i.e., MARC-SDF is address-based, while e-MARC is non-address-based[4]).

Up to our best knowledge, there is no explicit mathematical expressions to calculate the theoretical outage probability of MARC-SDF. Nevertheless, it is still meaningful to include MARC-SDF performance curves as a reference. The performance results with MARC-SDF, shown in Fig. 4, are all based on the Monte-Carlo method according to [24, eqs. (4)-(6)] with a modification of [36, eq. (12)], while all the curves for e-MARC are the theoretical results.

Deriving explicit mathematical expression of the outage probability with MARC-SDF is out of the scope of this paper; hence, we emphasize again that the conclusions for the superiority/inferiority of e-MARC related to MARC-SDF in the Asymmetric/Symmetric scenarios are based on simulations. Rigorous mathematical analyzes for the results shown in Fig. 4 are left as future study.

### C. Special cases

*1) Static intra links:* In the case that intra links are static (not suffering from fading), $AR$ and $BR$ links can be modeled as BSCs with constant crossover probabilities $p_A$ and $p_B$, respectively. This scenario may be exemplified by sensor networks where only the destination moves. In that case, averaging the $AR$ and $BR$ intra link variations over their pdfs can be eliminated from (21) and (22). Accordingly, the derivations of $\Pr(\varepsilon_1)$ and $\Pr(\varepsilon_2)$ can be reduced to

---

[3]The probabilities are computed at a system level [8].

[4]In practical applications, the value of $p_A * p_B$ can be directly estimated and exploited at the destination without requiring any overhead transmission from the relay [35, Section III-B].

$$\mathrm{Pr}(\varepsilon_1) = \frac{1}{\Gamma_{AD}} \int_0^\infty \int_{f_A^{-1}(\ddot\delta)}^{f_A^{-1}(1)} \exp\left(\frac{-f_B^{-1}(\ddot\omega)}{\Gamma_{BD}} - \frac{\gamma_{AD}}{\Gamma_{AD}}\right) d\gamma_{AD}\, p(\gamma_{R}$$

$$\mathrm{Pr}(\varepsilon_2) = \int_0^\infty \exp\left(\frac{-f_A^{-1}(1)}{\Gamma_{AD}} - \frac{f_B^{-1}(\ddot\delta)}{\Gamma_{BD}}\right) p(\gamma_{RD}) d\gamma_{RD},$$

$$(25)$$

where

$$\ddot\delta = H_b(p_A * p_B * \hat p_R(\gamma_{RD}))$$
$$\ddot\omega = \ddot\delta + 1 - f_A(\gamma_{AD}).$$

$$(26)$$

The results of the theoretical outage probabilities calculated in this special case are shown in Fig. 5. It can be clearly observed in Fig. 5 that the outage probability achieves the second-order diversity when $p_A = p_B = 0$, and matches the probability curve with perfect intra links in Fig. 3. When both intra links are imperfect but with relatively small crossover probabilities (e.g., when $p_A = p_B = 0.01$), it is found that the decay of the outage probability follows the second order diversity in the low $\Gamma_{iD}$ regime. However, the diversity order asymptotically converges to the first order as $\Gamma_{iD}$ increases. It should be noticed that for the case that $p_A \neq 0$ and $p_B \neq 0$, the relay remains silent with MARC-SDF or MARC-NC; however, with e-MARC, the erroneous estimates forwarded from the relay still contribute to reducing the outage probability.

In the case one of the intra links is perfect but the other one is imperfect, the helper's contribution, provided by the relay, depends on the quality of the imperfect link. This is because in (7a)-(7d) provided in Section III, the value of $p_A * p_B$ is a dominating factor that determines the size of the admissible rate region of $(\mathcal{R}_A, \mathcal{R}_B)$. Hence, $p_A$ dominates the value of $p_A * p_B$ if $p_B = 0$, and vice verse.

*2) DDEX e-MARC system [16]:* The derivation for the outage probability of the e-MARC system shown in Section III can further be used to evaluate the efficiency of the DDEX e-MARC system proposed by [16] where the erroneous estimates are also utilized. In [16], the information sequences $\mathbf{u}_i$ for $i \in \{A, B\}$ are first encoded by recursive systematic convolutional (RSC) codes, and then broadcasted from the source nodes using binary differential phase-shift-keying (DPSK) modulation.[5] To achieve low computational complexity and small latency, instead of performing fully-iterative decoding between the decoders of the accumulator (ACC) [37] and RSC code, the relay $R$ obtains the estimates $\widetilde{\mathbf{u}}_i$ of $\mathbf{u}_i$ by the DDEX detection strategy, where the relay simply extracts the systematic part output from the differential detector. The estimates $\widetilde{\mathbf{u}}_i$ for $i \in \{A, B\}$ are detected in error with a high probability because no error correction is performed at $R$, in exchange for saving battery and memory resources due to low computational complexity. The obtained estimates are XOR-network-coded at $R$ and forwarded to the destination $D$ for improving the FER performance.

[5]The accumulator (ACC) [37] followed by coherent PSK is equivalent to DPSK.
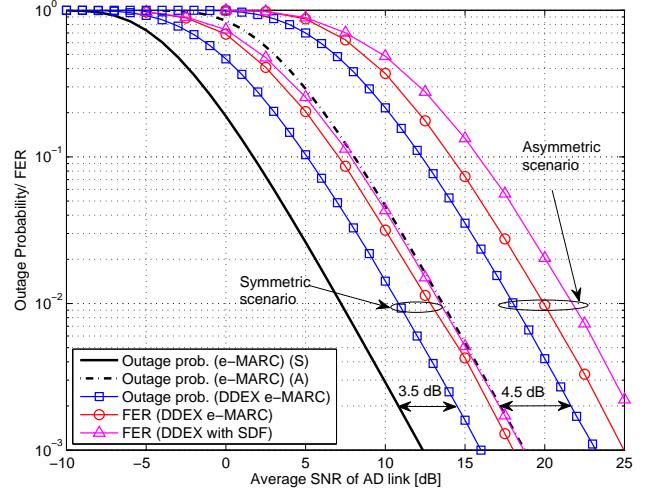


Fig. 6. Theoretical outage probabilities of DDEX e-MARC system [16]. Notations (S) and (A) denote Symmetric and Asymmetric scenarios listed in Table II, respectively. Select DF (SDF) strategy is same as that presented in [24].

TABLE III
PARAMETERS USED IN FER SIMULATIONS.

| | |
|---|---|
| Length of information sequence $(K)$ | 2048 bits |
| Generator polynomial of RSC code | $(07, 05)_8$ |
| Generator polynomial of ACC | $(03, 02)_8$ |
| Signaling scheme $\mathcal{E}_S$ | [16, Fig. 1] |
| Signaling scheme $\mathcal{E}_R$ | [16, Fig. 1] |
| Spectrum efficiency of $\mathcal{E}_S$ $(K/M)$ | 1/2 |
| Spectrum efficiency of $\mathcal{E}_R$ $(K/M)$ | 1/2 |
| Receiver $\mathcal{D}_R$ | DDEX |
| Receiver $\mathcal{D}_D$ | [16, Fig. 4] |
| Decoding algorithm | log-MAP |
| Decoding of $\mathcal{E}_S$ at $D$ | 10 iterations |
| Decoding between $\mathcal{E}_S$ and $\mathcal{E}_R$ at $D$ | 10 iterations |
| Interleavers | Random |

As shown in [16], DPSK modulation and differential detection are used at the source node and relay, respectively, and hence according to [38], the error probability of the *extracted* estimates of the information sequence is expressed as

$$p_i(\gamma_{iR}) = \frac{1}{2} \exp(-\gamma_{iR}), \qquad i \in \{A, B\}. \qquad (27)$$

The theoretical outage probability for the DDEX e-MARC system (i.e., the theoretical achievable FER performance of the system), is obtained by replacing (16) with (27) in (24). Results of outage probabilities in Symmetric and Asymmetric scenarios are demonstrated in Fig. 6 for comparison. The settings of the both scenarios are same as those in the subsection IV-B.

In Symmetric scenario, as shown in Fig. 6, the outage probability of DDEX e-MARC system is roughly 3.5 dB away from the outage probability of e-MARC that is independent of the signaling scheme. The gap is due to the relatively high $p_i$ value with DDEX. In Asymmetric scenario, the gap is further increased by 1 dB, resulting in a 4.5-dB gap from the outage probability of e-MARC. However, a large number of addition, multiplication and comparison operations can be eliminated on obtaining the estimates $\widetilde{\mathbf{u}}_i$, according to [39, Section 4.1].

The FER performance results of the DDEX e-MARC system obtained through simulations are also included in Fig. 6. Here FER is defined as follows: number of the transmission cycles where either one or both of the information sequences sent from the nodes $A$ and $B$ cannot successfully recovered at $D$ even with the help of $R$, divided by the total number of transmission cycles. The parameters used in the simulations are summarized in Table III. It is found from Fig. 6 that both in Symmetric and Asymmetric scenarios, there is a roughly 1.8-dB loss with the practical FER performance from the corresponding theoretical outage probabilities. The loss is because the theoretical outage probabilities are derived assuming the use of capacity-achieving codes in the the $iD$ and $RD$ links.

## V. IMPACT OF CORRELATION

In this section, we further extended our analysis to the e-MARC system where the correlation between two source nodes is taken into account. The correlation of source nodes is modeled by random bit-flipping with the flipping probability $p_s = \mathfrak{B}(\mathbf{u}_A, \mathbf{u}_B)$. The admissible rate region for the e-MARC system with the correlation $p_s$ between source nodes is analyzed in (40) in Appendix A. To investigate the impact of the source correlation $p_s$ and the network correlation $p_{nc} = p_A * p_B = \mathfrak{B}(\mathbf{u}_A \oplus \mathbf{u}_B, \widetilde{\mathbf{u}}_A \oplus \widetilde{\mathbf{u}}_B)$, three extreme scenarios: $(\Gamma_{AD}, \Gamma_{BD}, p_R) = $ (30 dB, -30 dB, 0), (30 dB, -30 dB, 0.5) and (-30 dB, -30 dB, 0.5) are investigated, respectively. The values of $\mathcal{R}_{ci}$ and $\mathcal{R}_{cR}$ are set to $1/2$.

### A. Source correlation $p_s$

We first focus on the impact of source correlation $p_s$ on the e-MARC outage probability. For the scenarios $(\Gamma_{AD}, \Gamma_{BD}, p_R) = $ (30 dB, -30 dB, 0) and (30 dB, -30 dB, 0.5), the soft channel values of the received signal vector $\mathbf{y}_{AD}$ are reliable while the values of $\mathbf{y}_{BD}$ are unreliable at the destination $D$. Even in this case, the information sequence $\mathbf{u}_B$ can still be recovered with a high probability if two source nodes are highly correlated. This is because when $\mathbf{u}_A$ and $\mathbf{u}_B$ are highly correlated, reliable *a priori* information for the recovery of $\mathbf{u}_B$ can be directly acquired from *extrinsic* information related to $\mathbf{u}_A$ during the decoding process. Hence, it can be concluded that, with or without the relay, when at least one of the direct links is reliable and the two source nodes are highly correlated, a very low probability can be achieved. This situation is demonstrated in Figs. 7(a) and 7(b), where the probability is shown as a function of $p_s$ and $p_{nc}$.

### B. Network correlation $p_{nc}$

Then, let us focus on the impact of the network correlation $p_{nc}$. Assuming $\mathbf{u}_A$ and $\mathbf{u}_B$ are uncorrelated, but $\mathbf{u}_A \oplus \mathbf{u}_B$ and $\widetilde{\mathbf{u}}_A \oplus \widetilde{\mathbf{u}}_B$ are fully correlated (i.e., $\mathbf{u}_A \oplus \mathbf{u}_B = \widetilde{\mathbf{u}}_A \oplus \widetilde{\mathbf{u}}_B$ and $p_{nc} = 0$). For the scenario $(\Gamma_{AD}, \Gamma_{BD}, p_R) = $ (30 dB, -30 dB, 0), the soft channel values of $\mathbf{y}_{AD}$ and $\mathbf{y}_{RD}$ at the destination are reliable while the values of $\mathbf{y}_{BD}$ are unreliable. In this scenario, $\mathbf{u}_A$ and $\mathbf{u}_R$ can be recovered with a high probability after the decoding of $\mathbf{y}_{AD}$ and $\mathbf{y}_{RD}$, respectively.

$\mathbf{u}_B$ can also be recovered with the aid of reliable *a priori* information using boxplus operation [40] on both *extrinsic* information corresponded to $\mathbf{u}_A$ and $\mathbf{u}_R$. However, for the scenario $(\Gamma_{AD}, \Gamma_{BD}, p_R) = $ (-30 dB, -30 dB, 0) with the same assumption, only the soft channel values of $\mathbf{y}_{RD}$ are reliable, and thus the recoveries of $\mathbf{u}_A$ and $\mathbf{u}_B$ require *apriori* information output from boxplus operation. Nevertheless, both *extrinsic* information related to $\mathbf{u}_A$ and $\mathbf{u}_B$ is unreliable with high probabilities, and hence, the output from boxplus operation is still unreliable for the decoding of $\mathbf{y}_{iD}$ for $i \in \{A, B\}$. Therefore, as shown in Fig. 7(c), the value of the probability cannot be reduced to a very small value, although both intra links and $RD$ link are perfect (i.e., $p_A = p_B = p_R = 0$).

## VI. CONCLUSION

We have derived the outage probability for the e-MARC system. The theoretical outage probabilities of MARC-NC [8] and MARC-SDF [24] were also included for comparisons in Symmetric/Asymmetric scenarios listed in Table II. It has been observed through simulations that the outage probability of MARC-NC is inferior to that of e-MARC. Moreover, it has been found through simulations that in Asymmetric scenario where one of the source nodes is far away from both the relay and the destination, e-MARC performs better than MARC-SDF. However, in Symmetric scenario, e-MARC is inferior to MARC-SDF.

We have further applied the derivation process of the outage probabilities to two special cases: 1) static intra links and 2) the previously proposed DDEX e-MARC system [16]. According to the numerical results shown in case 1), we verified that erroneous estimates received at the relay is useful for the recovery of the information sequences at the destination. To evaluate the DDEX e-MARC system, comparisons are provided between the e-MARC outage probability and the outage probability of the DDEX e-MARC system in case 2). It was found that a 3.5 to 4.5-dB loss is in exchange for a significant reduction in computational complexity. Finally, we recognized that for the case two source nodes are highly correlated, the source correlation can be exploited to improve the e-MARC outage performance even if only one of the direct links is reliable.

## APPENDIX A
### DERIVATION OF (7a)-(7d)

We start the derivation of the results of (7a)-(7d) with the general equivalent system model of e-MARC shown in Fig. 8, where source nodes $A$ and $B$ are assumed to be correlated. Variables $e_A$, $e_B$, $e_R$ and $e_s$ are i.i.d. binary random variables with $\Pr(e_A = 1) = p_A$, $\Pr(e_B = 1) = p_B$, $\Pr(e_R = 1) = p_R$ and $\Pr(e_s = 1) = p_s$, respectively. According to the definition, the mutual information $I(\mathbf{u}_R; \hat{\mathbf{u}}_R)$ is

$$I(\mathbf{u}_R; \hat{\mathbf{u}}_R) = H(\hat{\mathbf{u}}_R) - H(\hat{\mathbf{u}}_R | \mathbf{u}_R). \quad (28)$$
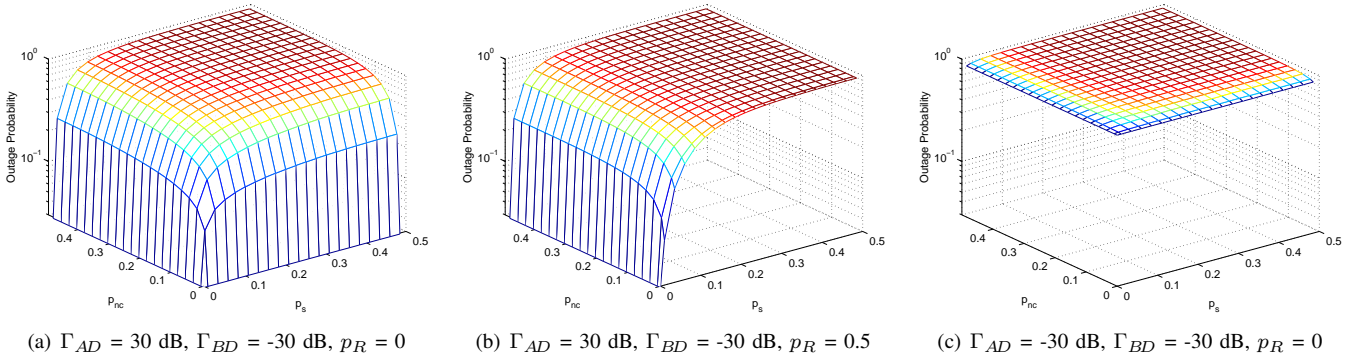
(a) $\Gamma_{AD}$ = 30 dB, $\Gamma_{BD}$ = -30 dB, $p_R = 0$     (b) $\Gamma_{AD}$ = 30 dB, $\Gamma_{BD}$ = -30 dB, $p_R = 0.5$     (c) $\Gamma_{AD}$ = -30 dB, $\Gamma_{BD}$ = -30 dB, $p_R = 0$

Fig. 7. Impacts of source correlation $p_s$ and network correlation $p_{nc}$ on outage probability of e-MARC. Here $\mathcal{R}_{ci} = \mathcal{R}_{cR} = 1/2$.
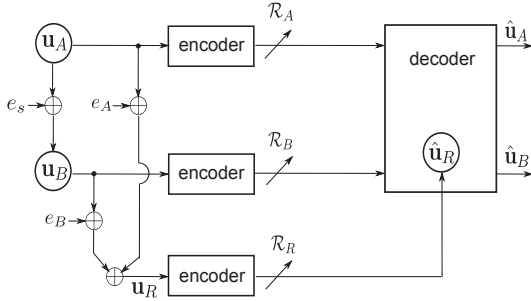


Fig. 8. Generalized equivalent model of e-MARC, where source correlation is taken into account.

Then, given the model shown in Fig. 8, $I(\mathbf{u}_R; \hat{\mathbf{u}}_R)$ can be further expressed as follows

$$I(\mathbf{u}_R; \hat{\mathbf{u}}_R) = H(\underbrace{\mathbf{u}_A \oplus e_A}_{\tilde{\mathbf{u}}_A} \oplus \underbrace{\mathbf{u}_B \oplus e_B}_{\tilde{\mathbf{u}}_B} \oplus e_R) - H_b(p_R)$$
$$= H(\underbrace{\mathbf{u}_A \oplus e_A}_{\tilde{\mathbf{u}}_A} \oplus \underbrace{\mathbf{u}_A \oplus e_s \oplus \mathbf{u}_B}_{\tilde{\mathbf{u}}_B} \oplus e_R) - H_b(p_R)$$
$$= H(e_A \oplus e_B \oplus e_R \oplus e_s) - H_b(p_R)$$
$$= H_b(p_A * p_B * p_R * p_s) - H_b(p_R), \quad (29)$$

where the operation $\alpha * \beta$ is defined as $\alpha(1-\beta) + \beta(1-\alpha)$, and $H_b(\cdot)$ denotes the binary entropy function [29]. For the sake of notation simplicity, we defined $\mu$ as $\mu = H(\hat{\mathbf{u}}_R) = H_b(p_A * p_B * p_R * p_s)$. Then, by using the chain rule, the joint entropy $H(\mathbf{u}_A, \mathbf{u}_B, \mathbf{u}_R, \hat{\mathbf{u}}_R)$ can be represented as

$$H(\mathbf{u}_A, \mathbf{u}_B, \mathbf{u}_R, \hat{\mathbf{u}}_R) = H(\mathbf{u}_A, \mathbf{u}_B) + H(\mathbf{u}_R|\mathbf{u}_A, \mathbf{u}_B)$$
$$+ H(\hat{\mathbf{u}}_R|\mathbf{u}_A, \mathbf{u}_B, \mathbf{u}_R) \quad (30a)$$
$$= H(\hat{\mathbf{u}}_R) + H(\mathbf{u}_A, \mathbf{u}_B|\hat{\mathbf{u}}_R)$$
$$+ H(\mathbf{u}_R|\mathbf{u}_A, \mathbf{u}_B, \hat{\mathbf{u}}_R). \quad (30b)$$

Hence, the conditional entropy $H(\mathbf{u}_A, \mathbf{u}_B|\hat{\mathbf{u}}_R)$ is expressed with the combination of (30a) and (30b), as

$$H(\mathbf{u}_A, \mathbf{u}_B|\hat{\mathbf{u}}_R) = H(\mathbf{u}_A, \mathbf{u}_B) + H(\mathbf{u}_R|\mathbf{u}_A, \mathbf{u}_B)$$
$$+ H(\hat{\mathbf{u}}_R|\mathbf{u}_A, \mathbf{u}_B, \mathbf{u}_R) - H(\hat{\mathbf{u}}_R)$$
$$- H(\mathbf{u}_R|\mathbf{u}_A, \mathbf{u}_B, \hat{\mathbf{u}}_R). \quad (31)$$

Also, the conditional mutual information $I(\mathbf{u}_R; \hat{\mathbf{u}}_R|\mathbf{u}_A, \mathbf{u}_B)$ can be expressed by the chain rule, as

$$I(\mathbf{u}_R; \hat{\mathbf{u}}_R|\mathbf{u}_A, \mathbf{u}_B) = H(\mathbf{u}_R|\mathbf{u}_A, \mathbf{u}_B) - H(\mathbf{u}_R|\mathbf{u}_A, \mathbf{u}_B, \hat{\mathbf{u}}_R)$$
$$= H(\hat{\mathbf{u}}_R|\mathbf{u}_A, \mathbf{u}_B) - H(\hat{\mathbf{u}}_R|\mathbf{u}_A, \mathbf{u}_B, \mathbf{u}_R). \quad (32)$$

By substituting $H(\mathbf{u}_R|\mathbf{u}_A, \mathbf{u}_B)$ of (32) into (31), $H(\mathbf{u}_A, \mathbf{u}_B|\hat{\mathbf{u}}_R)$ can be rewritten as

$$H(\mathbf{u}_A, \mathbf{u}_B|\hat{\mathbf{u}}_R) = H(\mathbf{u}_A, \mathbf{u}_B) + H(\hat{\mathbf{u}}_R|\mathbf{u}_A, \mathbf{u}_B) - H(\hat{\mathbf{u}}_R) \quad (33)$$

where the conditional entropy $H(\hat{\mathbf{u}}_R|\mathbf{u}_A, \mathbf{u}_B)$ is calculated as

$$H(\hat{\mathbf{u}}_R|\mathbf{u}_A, \mathbf{u}_B) = H(\mathbf{u}_A \oplus e_A \oplus \mathbf{u}_B \oplus e_B \oplus e_R|\mathbf{u}_A, \mathbf{u}_B)$$
$$= H(e_A \oplus e_B \oplus e_R). \quad (34)$$

Therefore, $H(\mathbf{u}_A, \mathbf{u}_B|\hat{\mathbf{u}}_R)$ shown in the third inequality of (6) can be obtained by substituting (34) into (33), as

$$H(\mathbf{u}_A, \mathbf{u}_B|\hat{\mathbf{u}}_R) = H(\mathbf{u}_A, \mathbf{u}_B) + H(e_A \oplus e_B \oplus e_R) - H(\hat{\mathbf{u}}_R)$$
$$= 1 + H_b(p_s) + H_b(p_A * p_B * p_R) - \mu. \quad (35)$$

Again, let $\delta_s = H_b(p_s) + H_b(p_A * p_B * p_R) - \mu$ for simplicity. Since the conditional entropy $H(\mathbf{u}_A, \mathbf{u}_B|\hat{\mathbf{u}}_R)$ in (35) can also alternatively be expressed by the chain rule, as

$$H(\mathbf{u}_A, \mathbf{u}_B|\hat{\mathbf{u}}_R) = H(\mathbf{u}_B|\mathbf{u}_A, \hat{\mathbf{u}}_R) + H(\mathbf{u}_A|\hat{\mathbf{u}}_R) \quad (36a)$$
$$= H(\mathbf{u}_A|\mathbf{u}_B, \hat{\mathbf{u}}_R) + H(\mathbf{u}_B|\hat{\mathbf{u}}_R). \quad (36b)$$

Since the sequence $\hat{\mathbf{u}}_R$ is composed of $\mathbf{u}_A$, the conditional entropy $H(\mathbf{u}_A|\hat{\mathbf{u}}_R)$ in (36a) can be calculated as

$$H(\mathbf{u}_A|\hat{\mathbf{u}}_R) = H(\mathbf{u}_A|\mathbf{u}_A \oplus e_A \oplus \mathbf{u}_B \oplus e_B \oplus e_R)$$
$$= H(e_A \oplus \mathbf{u}_A \oplus e_s \oplus \mathbf{u}_B \oplus e_R)$$
$$= 1. \quad (37)$$

Therefore, we can obtain $H(\mathbf{u}_B|\mathbf{u}_A, \hat{\mathbf{u}}_R)$, shown in the second inequality of (6), by substituting (35) and (37) into (36a), as

$$H(\mathbf{u}_B|\mathbf{u}_A, \hat{\mathbf{u}}_R) = \underbrace{H(\mathbf{u}_A, \mathbf{u}_B|\hat{\mathbf{u}}_R)}_{1+\delta_s} - \underbrace{H(\mathbf{u}_A|\hat{\mathbf{u}}_R)}_{1}$$
$$= \delta_s. \quad (38)$$

The conditional entropy $H(\mathbf{u}_A|\mathbf{u}_B, \hat{\mathbf{u}}_R)$ shown in the first inequality of (6) is also calculated in the same way, and the result is

$$H(\mathbf{u}_A|\mathbf{u}_B, \hat{\mathbf{u}}_R) = \delta_s. \tag{39}$$

A set of inequalities is obtained by combining (29), (35), (38) and (39), as

$$\begin{aligned}
\mathcal{R}_A &\geq \delta_s, \\
\mathcal{R}_B &\geq \delta_s, \\
\mathcal{R}_A + \mathcal{R}_B &\geq 1 + \delta_s, \\
\mathcal{R}_R &\geq \mu - H_b(p_R).
\end{aligned} \tag{40}$$

For the case that the two source nodes are uncorrelated (i.e., $p_s = 0.5$), $\mu = 1$ and $\delta_s = \delta = H_b(p_A * p_B * p_R)$, which leads (40) into (7a)-(7d).

## APPENDIX B
## DIVISIONS OF INTEGRALS (21) AND (22)

As shown in (16) and (18), the values of $\hat{p}_i(\gamma_{iR})$ and $\hat{p}_R(\gamma_{RD})$ become zero as the SNR $\gamma_{iR}$ and $\gamma_{RD}$ excess over the threshold value, and thus, the domain of the integral shown in (23) can be divided into eight intervals according to the threshold value $\gamma_A^*$, $\gamma_B^*$ and $\gamma_R^*$, as

$$\Pr(\varepsilon_1) = \mathfrak{I}[g_1; V] = \sum_{j=1}^{8} \mathfrak{I}[g_1; V_j]$$
$$\Pr(\varepsilon_2) = \mathfrak{I}[g_2; V] = \sum_{j=1}^{8} \mathfrak{I}[g_2; V_j], \tag{41}$$

where

$$\begin{aligned}
V_1 &= \{(\gamma_{AR}, \gamma_{BR}, \gamma_{RD}) : \gamma_{AR} \in \mathbb{A}^+, \gamma_{BR} \in \mathbb{B}^+, \gamma_{RD} \in \mathbb{C}^+\} \\
V_2 &= \{(\gamma_{AR}, \gamma_{BR}, \gamma_{RD}) : \gamma_{AR} \in \mathbb{A}^+, \gamma_{BR} \in \mathbb{B}^-, \gamma_{RD} \in \mathbb{C}^+\} \\
V_3 &= \{(\gamma_{AR}, \gamma_{BR}, \gamma_{RD}) : \gamma_{AR} \in \mathbb{A}^-, \gamma_{BR} \in \mathbb{B}^+, \gamma_{RD} \in \mathbb{C}^+\} \\
V_4 &= \{(\gamma_{AR}, \gamma_{BR}, \gamma_{RD}) : \gamma_{AR} \in \mathbb{A}^-, \gamma_{BR} \in \mathbb{B}^-, \gamma_{RD} \in \mathbb{C}^+\} \\
V_5 &= \{(\gamma_{AR}, \gamma_{BR}, \gamma_{RD}) : \gamma_{AR} \in \mathbb{A}^+, \gamma_{BR} \in \mathbb{B}^+, \gamma_{RD} \in \mathbb{C}^-\} \\
V_6 &= \{(\gamma_{AR}, \gamma_{BR}, \gamma_{RD}) : \gamma_{AR} \in \mathbb{A}^+, \gamma_{BR} \in \mathbb{B}^-, \gamma_{RD} \in \mathbb{C}^-\} \\
V_7 &= \{(\gamma_{AR}, \gamma_{BR}, \gamma_{RD}) : \gamma_{AR} \in \mathbb{A}^-, \gamma_{BR} \in \mathbb{B}^+, \gamma_{RD} \in \mathbb{C}^-\} \\
V_8 &= \{(\gamma_{AR}, \gamma_{BR}, \gamma_{RD}) : \gamma_{AR} \in \mathbb{A}^-, \gamma_{BR} \in \mathbb{B}^-, \gamma_{RD} \in \mathbb{C}^-\}.
\end{aligned} \tag{42}$$

Here, the sets $\mathbb{A}^-$, $\mathbb{A}^+$, $\mathbb{B}^-$, $\mathbb{B}^+$, $\mathbb{C}^-$ and $\mathbb{C}^+$ are defined as

$$\begin{aligned}
\mathbb{A}^- &= [0, \gamma_A^*), & \mathbb{A}^+ &= [\gamma_A^*, \infty) \\
\mathbb{B}^- &= [0, \gamma_B^*), & \mathbb{B}^+ &= [\gamma_B^*, \infty) \\
\mathbb{C}^- &= [0, \gamma_R^*), & \mathbb{C}^+ &= [\gamma_R^*, \infty).
\end{aligned} \tag{43}$$

The integrals of (21) and (22) with respect to each interval listed in (42) are expressed in (44) and (45), respectively. The arguments $\hat{\delta}_j$ and $\hat{\omega}_j$ corresponding to each interval in (44) and (45) are summarized in Table IV.

## REFERENCES

[1] G. Kramer and A. van Wijngaarden, "On the white Gaussian multiple-access relay channel," in *Proc. IEEE Int. Symp. Inform. Theory*, 2000, p. 40.

[2] Y. Zhang and Z. Zhang, "Joint network-channel coding with rateless code over multiple access relay system," *IEEE Trans. Wireless Commun.*, vol. 12, no. 1, pp. 320–332, Jan. 2013.

[3] Y. Li, G. Song, and L. Wang, "Design of joint network-low density parity check codes based on the exit charts," *IEEE Commun. Lett.*, vol. 13, no. 8, pp. 600 –602, Aug. 2009.

[4] S. Tang, J. Cheng, C. Sun, and R. Miura, "Joint channel and network decoding for XOR-based relay in multi-access channel," *IEICE Trans. Commun.*, vol. E92-B, no. 11, pp. 3470–3477, Nov. 2009.

[5] C. Hausl and P. Dupraz, "Joint network-channel coding for the multiple-access relay channel," in *Proc. IEEE Commun. Soc. Sensor and Ad Hoc Commun. and Netw.*, vol. 3, sept. 2006, pp. 817–822.

[6] X. Xu, M. Flanagan, C. Koller, and N. Goertz, "A shared-relay cooperative diversity scheme based on joint channel and network coding," in *Proc. Int. Symp. Inform. Theory Its Appl.*, dec. 2008, pp. 1–6.

[7] M. Hernaez, P. Crespo, and J. Del Ser, "On the design of a novel joint network-channel coding scheme for the multiple access relay channel," *IEEE J. Sel. Areas Commun.*, vol. 31, no. 8, pp. 1368–1378, Aug. 2013.

[8] D. Woldegebreal and H. Karl, "Multiple-access relay channel with network coding and non-ideal source-relay channels," in *Proc. Int. Symp. Wireless Commun. Syst.*, 2007, pp. 732–736.

[9] S. Yang and R. Koetter, "Network coding over a noisy relay: a belief propagation approach," in *Proc. IEEE Int. Symp. Inform. Theory*, 2007, pp. 801–804.

[10] H. Sneessens and L. Vandendorpe, "Soft decode and forward improves cooperative communications," in *Proc. IEEE Int. Workshop Computat. Adv. Multi-Sensor Adaptive Process*, 2005, pp. 157–160.

[11] Y. Li, B. Vucetic, T. Wong, and M. Dohler, "Distributed turbo coding with soft information relaying in multihop relay networks," *IEEE J. Sel. Areas Commun.*, vol. 24, no. 11, pp. 2040–2050, 2006.

[12] H. Sneessens, J. Louveaux, and L. Vandendorpe, "Turbo-coded decode-and-forward strategy resilient to relay errors," in *Proc. IEEE Int. Conf. Acoustics, Speech Signal Process*, 2008, pp. 3213 –3216.

[13] K. Lee and L. Hanzo, "MIMO-assisted hard versus soft decoding-and-forwarding for network coding aided relaying systems," *IEEE Trans. Wireless Commun.*, vol. 8, no. 1, pp. 376–385, 2009.

[14] M. Xiao and T. Aulin, "Optimal decoding and performance analysis of a noisy channel network with network coding," *IEEE Trans. Commun.*, vol. 57, no. 5, pp. 1402–1412, 2009.

[15] T.-W. Y. Yune, D. Kim, and G.-H. Im, "Opportunistic network-coded cooperative transmission with demodulate-and-forward protocol in wireless channels," *IEEE Trans Commun.*, vol. 59, no. 7, pp. 1791–1795, 2011.

[16] P.-S. Lu and T. Matsumoto, "Energy-efficient techniques allowing intra-link errors for block-fading multiple access relaying," in *Proc. IEEE 22nd Int. Symp. Pers. Indoor and Mobile Radio Commun.*, Sept 2011, pp. 1687–1691.

[17] G. Zeitler, G. Bauch, and J. Widmer, "Quantize-and-forward schemes for the orthogonal multiple-access relay channel," *IEEE Trans. Commun.*, vol. 60, no. 4, pp. 1148–1158, 2012.

[18] X.-T. Vu, M. Di Renzo, and P. Duhamel, "Iterative network/channel decoding for the noisy multiple-access relay channel (MARC)," in *Proc. IEEE Int. Conf. Acoustics, Speech and Signal Process*, 2012, pp. 2901–2904.

[19] Y. Yin, R. Pyndiah, and K. Amis, "Performance of turbo product codes on the multiple-access relay channel with relatively poor source-relay links," in *Proc. IEEE 13th Int. Workshop Signal Process Adv. Wireless Commun.*, 2012, pp. 419–423.

[20] K. Q. Huynh and T. Aulin, "Improved iterative decoders for turbo-coded decode-and-forward relay channels," in *Proc. 2012 IEEE Veh. Technol. Conf.*, 2012, pp. 1–5.

[21] A. Mohamad, R. Visoz, and A. O. Berthet, "Outage analysis of various cooperative strategies for the multiple access multiple relay channel," in *Proc. 2013 IEEE 24th Int. Symp. Pers. Indoor Mobile Radio Commun.*, Sept 2013, pp. 1321–1326.

[22] A. Mohamad, R. Visoz, and A. Berthet, "Outage achievable rate analysis for the non orthogonal multiple access multiple relay channel," in *Proc. 2013 IEEE Wireless Commun. Netw. Conf. Workshop*, April 2013, pp. 160–165.

[23] Q. Meng and C. Wang, "Outage probability analysis of multiple-access relay channel with network coding and relay selection," *J. Inform. Comput. Sci.*, pp. 829–837, 2013. [Online]. Available: www.joics.com.

TABLE IV
ARGUMENTS OF FUNCTIONS $f_A^{-1}(\cdot)$ AND $f_B^{-1}(\cdot)$ IN (44) AND (45).

| $\hat{\delta}_1$ | $H_b(0*0*0)$ | $\hat{\omega}_1$ | $\hat{\delta}_1 + 1 - f_A(\gamma_{AD})$ |
|---|---|---|---|
| $\hat{\delta}_2$ | $H_b(0*\tilde{p}_B(\gamma_{BR})*0)$ | $\hat{\omega}_2$ | $\hat{\delta}_2 + 1 - f_A(\gamma_{AD})$ |
| $\hat{\delta}_3$ | $H_b(\tilde{p}_A(\gamma_{AR})*0*0)$ | $\hat{\omega}_3$ | $\hat{\delta}_3 + 1 - f_A(\gamma_{AD})$ |
| $\hat{\delta}_4$ | $H_b(\tilde{p}_A(\gamma_{AR})*\tilde{p}_B(\gamma_{BR})*0)$ | $\hat{\omega}_4$ | $\hat{\delta}_4 + 1 - f_A(\gamma_{AD})$ |
| $\hat{\delta}_5$ | $H_b(0*0*\tilde{p}_R(\gamma_{RD}))$ | $\hat{\omega}_5$ | $\hat{\delta}_5 + 1 - f_A(\gamma_{AD})$ |
| $\hat{\delta}_6$ | $H_b(0*\tilde{p}_B(\gamma_{BR})*\tilde{p}_R(\gamma_{RD}))$ | $\hat{\omega}_6$ | $\hat{\delta}_6 + 1 - f_A(\gamma_{AD})$ |
| $\hat{\delta}_7$ | $H_b(\tilde{p}_A(\gamma_{AR})*0*\tilde{p}_R(\gamma_{RD}))$ | $\hat{\omega}_7$ | $\hat{\delta}_7 + 1 - f_A(\gamma_{AD})$ |
| $\hat{\delta}_8$ | $H_b(\tilde{p}_A(\gamma_{AR})*\tilde{p}_B(\gamma_{BR})*\tilde{p}_R(\gamma_{RD}))$ | $\hat{\omega}_8$ | $\hat{\delta}_8 + 1 - f_A(\gamma_{AD})$ |

[24] O. Iscan and C. Hausl, "Iterative network and channel decoding for the relay channel with multiple sources," in *Proc. IEEE Veh. Technol. Conf.*, sept. 2011, pp. 1–5.

[25] D. Slepian and J. Wolf, "Noiseless coding of correlated information sources," *IEEE Trans. Inf. Theory,*, vol. 19, no. 4, pp. 471–480, 1973.

[26] M. Cheng, K. Anwar, and T. Matsumoto, "Outage probability of a relay strategy allowing intra-link errors utilizing slepian-wolf theorem," *EURASIP J. Adv. Signal Process*, vol. 34, 2013.

[27] X. Zhou, P.-S. Lu, K. Anwar, and T. Matsumoto, "Correlated sources transmission in orthogonal multiple access relay channel: Theoretical analysis and performance evaluation," *IEEE Trans. Wireless Comm.*, vol. 13, no. 3, pp. 1424–1435, March 2014.

[28] A. Gamal and Y. Kim, "Network Information theory," *Cambridge University Press*, 2011.

[29] T. M. Cover and J. A. Thomas, "Elements of Information Theory 2nd Edition," *USA: John Wiley & Sons, Inc.*, 2006.

[30] J. Garcia-Frias and Y. Zhao, "Near-Shannon/Slepian-Wolf performance for unknown correlated sources over AWGN channels," *IEEE Trans. Commun.*, vol. 53, no. 4, pp. 555–559, 2005.

[31] C. Tian, J. Chen, S. Diggavi, and S. Shamai, "Optimality and approximate optimality of source-channel separation in networks," *IEEE Trans on Inform. Theory*, vol. 60, no. 2, pp. 904–918, Feb 2014.

[32] Y. Murin, R. Dabora, and D. Gunduz, "Source-channel coding theorems for the multiple-access relay channel," *IEEE Trans on Inform. Theory*, vol. 59, no. 9, pp. 5446–5465, Sept 2013.

[33] R. J. McEliece, "The Theory of Information and Coding, 2nd ed." *Cambridge University Press*, 2002.

[34] L. Shampine, "Matlab program for quadrature in 2d," *Applied Mathematics and Computation*, vol. 202, no. 1, pp. 266–274, 2008.

[35] P.-S. Lu, X. Zhou, K. Anwar, and T. Matsumoto, "Joint adaptive network-channel coding for energy-efficient multiple-access relaying," *IEEE Trans. Veh. Tech.*, vol. 63, no. 5, pp. 2298–2305, Jun 2014.

[36] L. Sankaranarayanan, G. Kramer, and N. B. Mandayam, "Hierarchical sensor networks: capacity bounds and cooperative strategies using the multiple-access relay channel model," in *Proc. 1st Annual IEEE Commun. Soc. Conf. Sensor Ad Hoc Commun. Netw.*, Oct., pp. 191–199.

[37] S. ten Brink and G. Kramer, "Design of repeat-accumulate codes for iterative detection and decoding," *IEEE Trans. Signal Process.*, vol. 51, no. 11, pp. 2764 – 2772, nov 2003.

[38] G. Maral and M. Bousquet, "Satellite Communications systems," *John Wiley and Sons*, 2009.

[39] P. Robertson, E. Villebrun, and P. Hoeher, "A comparison of optimal and sub-optimal map decoding algorithms operating in the log domain," in *Proc. IEEE Int. Conf. Commun.*, vol. 2, jun 1995, pp. 1009 –1013 vol.2.

[40] J. Hagenauer, E. Offer, and L. Papke, "Iterative decoding of binary block and convolutional codes," *IEEE Trans. Inf. Theory,*, vol. 42, no. 2, pp. 429–445, Mar 1996.

**Pen-Shun Lu** (S'09) received the B.S. degree in electrical engineering from National Sun Yat-Sen University (NSYSU), Taiwan, in 2003 and the M.Sc in wireless communications from the University of Southampton, UK, in 2007. Currently he is pursuing the PhD degrees in University of Oulu, Finland and Japan Advanced Institute of Science and Technology (JAIST), Japan. His current research interests include joint source and channel coding, distributed coding, iterative detection and cooperative communications.
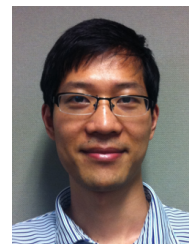
**Xiaobo Zhou** (S'11−M'13) recieved the B.Sc. in Electronic Information Science and Technology from University of Science and Technology of China (USTC), Hefei, China, in 2007, the M.E. in Computer Application Technology from Graduate University of Chinese Academy of Science (GU-CAS), Beijing, China, in 2010, and the Ph.D. degree from School of Information Science, Japan Advanced Institute of Science and Technology (JAIST), Ishikawa, Japan, in 2013. Now he is with Department of Communications Engineering, University of Oulu, Finland as a researcher. His research interests include coding techniques, joint source-channel coding, cooperative wireless communications and network information theory.

$$\Im[g_1;V_1] = \frac{1}{\Gamma_{AD}} \exp\left(-\frac{\gamma_R^*}{\Gamma_{RD}} - \frac{\gamma_A^*}{\Gamma_{AR}} - \frac{\gamma_B^*}{\Gamma_{BR}}\right) \int_{f_A^{-1}(\hat\delta_1)}^{f_A^{-1}(1)} \exp\left(\frac{-f_B^{-1}(\hat\omega_1)}{\Gamma_{BD}} - \frac{\gamma_{AD}}{\Gamma_{AD}}\right) d\gamma_{AD}$$

$$\Im[g_1;V_2] = \frac{1}{\Gamma_{AD}\Gamma_{BR}} \exp\left(-\frac{\gamma_R^*}{\Gamma_{RD}} - \frac{\gamma_A^*}{\Gamma_{AR}}\right) \int_0^{\gamma_B^*}\int_{f_A^{-1}(\hat\delta_2)}^{f_A^{-1}(1)} \exp\left(\frac{-f_B^{-1}(\hat\omega_2)}{\Gamma_{BD}} - \frac{\gamma_{AD}}{\Gamma_{AD}} - \frac{\gamma_{BR}}{\Gamma_{BR}}\right) d\gamma_{AD}\,d\gamma_{BR}$$

$$\Im[g_1;V_3] = \frac{1}{\Gamma_{AD}\Gamma_{AR}} \exp\left(-\frac{\gamma_R^*}{\Gamma_{RD}} - \frac{\gamma_B^*}{\Gamma_{BR}}\right) \int_0^{\gamma_A^*}\int_{f_A^{-1}(\hat\delta_3)}^{f_A^{-1}(1)} \exp\left(\frac{-f_B^{-1}(\hat\omega_3)}{\Gamma_{BD}} - \frac{\gamma_{AD}}{\Gamma_{AD}} - \frac{\gamma_{AR}}{\Gamma_{AR}}\right) d\gamma_{AD}\,d\gamma_{AR}$$

$$\Im[g_1;V_4] = \frac{1}{\Gamma_{AD}\Gamma_{AR}\Gamma_{BR}} \exp\left(-\frac{\gamma_R^*}{\Gamma_{RD}}\right) \int_0^{\gamma_B^*}\int_0^{\gamma_A^*}\int_{f_A^{-1}(\hat\delta_4)}^{f_A^{-1}(1)} \exp\left(\frac{-f_B^{-1}(\hat\omega_4)}{\Gamma_{BD}} - \frac{\gamma_{AD}}{\Gamma_{AD}} - \frac{\gamma_{AR}}{\Gamma_{AR}} - \frac{\gamma_{BR}}{\Gamma_{BR}}\right) d\gamma_{AD}\,d\gamma_{AR}\,d\gamma_{BR}$$

$$\Im[g_1;V_5] = \frac{1}{\Gamma_{AD}\Gamma_{RD}} \exp\left(-\frac{\gamma_A^*}{\Gamma_{AR}} - \frac{\gamma_B^*}{\Gamma_{BR}}\right) \int_0^{\gamma_R^*}\int_{f_A^{-1}(\hat\delta_5)}^{f_A^{-1}(1)} \exp\left(\frac{-f_B^{-1}(\hat\omega_5)}{\Gamma_{BD}} - \frac{\gamma_{AD}}{\Gamma_{AD}} - \frac{\gamma_{RD}}{\Gamma_{RD}}\right) d\gamma_{AD}\,d\gamma_{RD}$$

$$\Im[g_1;V_6] = \frac{1}{\Gamma_{AD}\Gamma_{RD}\Gamma_{BR}} \exp\left(-\frac{\gamma_A^*}{\Gamma_{AR}}\right) \int_0^{\gamma_R^*}\int_0^{\gamma_B^*}\int_{f_A^{-1}(\hat\delta_6)}^{f_A^{-1}(1)} \exp\left(\frac{-f_B^{-1}(\hat\omega_6)}{\Gamma_{BD}} - \frac{\gamma_{AD}}{\Gamma_{AD}} - \frac{\gamma_{BR}}{\Gamma_{BR}} - \frac{\gamma_{RD}}{\Gamma_{RD}}\right) d\gamma_{AD}\,d\gamma_{BR}\,d\gamma_{RD}$$

$$\Im[g_1;V_7] = \frac{1}{\Gamma_{AD}\Gamma_{RD}\Gamma_{AR}} \exp\left(-\frac{\gamma_B^*}{\Gamma_{BR}}\right) \int_0^{\gamma_R^*}\int_0^{\gamma_A^*}\int_{f_A^{-1}(\hat\delta_7)}^{f_A^{-1}(1)} \exp\left(\frac{-f_B^{-1}(\hat\omega_7)}{\Gamma_{BD}} - \frac{\gamma_{AD}}{\Gamma_{AD}} - \frac{\gamma_{AR}}{\Gamma_{AR}} - \frac{\gamma_{RD}}{\Gamma_{RD}}\right) d\gamma_{AD}\,d\gamma_{AR}\,d\gamma_{RD}$$

$$\Im[g_1;V_8] = \frac{1}{\Gamma_{AD}\Gamma_{RD}\Gamma_{AR}\Gamma_{BR}} \int_0^{\gamma_R^*}\int_0^{\gamma_B^*}\int_0^{\gamma_A^*}\int_{f_A^{-1}(\hat\delta_8)}^{f_A^{-1}(1)} \exp\left(\frac{-f_B^{-1}(\hat\omega_8)}{\Gamma_{BD}} - \frac{\gamma_{AD}}{\Gamma_{AD}} - \frac{\gamma_{AR}}{\Gamma_{AR}} - \frac{\gamma_{BR}}{\Gamma_{BR}} - \frac{\gamma_{RD}}{\Gamma_{RD}}\right) d\gamma_{AD}\,d\gamma_{AR}\,d\gamma_{BR}\,d\gamma_{RD}$$

$$(44)$$

$$\Im[g_2;V_1] = \exp\left(\frac{-f_A^{-1}(1)}{\Gamma_{AD}} - \frac{\gamma_R^*}{\Gamma_{RD}} - \frac{\gamma_A^*}{\Gamma_{AR}} - \frac{\gamma_B^*}{\Gamma_{BR}}\right)$$

$$\Im[g_2;V_2] = \frac{1}{\Gamma_{BR}} \exp\left(\frac{-f_A^{-1}(1)}{\Gamma_{AD}} - \frac{\gamma_R^*}{\Gamma_{RD}} - \frac{\gamma_A^*}{\Gamma_{AR}}\right) \int_0^{\gamma_B^*} \exp\left(\frac{-f_B^{-1}(\hat\delta_2)}{\Gamma_{BD}} - \frac{\gamma_{BR}}{\Gamma_{BR}}\right) d\gamma_{BR}$$

$$\Im[g_2;V_3] = \frac{1}{\Gamma_{AR}} \exp\left(\frac{-f_A^{-1}(1)}{\Gamma_{AD}} - \frac{\gamma_R^*}{\Gamma_{RD}} - \frac{\gamma_B^*}{\Gamma_{BR}}\right) \int_0^{\gamma_A^*} \exp\left(\frac{-f_B^{-1}(\hat\delta_3)}{\Gamma_{BD}} - \frac{\gamma_{AR}}{\Gamma_{AR}}\right) d\gamma_{AR}$$

$$\Im[g_2;V_4] = \frac{1}{\Gamma_{AR}\Gamma_{BR}} \exp\left(\frac{-f_A^{-1}(1)}{\Gamma_{AD}} - \frac{\gamma_R^*}{\Gamma_{RD}}\right) \int_0^{\gamma_B^*}\int_0^{\gamma_A^*} \exp\left(\frac{-f_B^{-1}(\hat\delta_4)}{\Gamma_{BD}} - \frac{\gamma_{AR}}{\Gamma_{AR}} - \frac{\gamma_{BR}}{\Gamma_{BR}}\right) d\gamma_{AR}\,d\gamma_{BR}$$

$$\Im[g_2;V_5] = \frac{1}{\Gamma_{RD}} \exp\left(\frac{-f_A^{-1}(1)}{\Gamma_{AD}} - \frac{\gamma_A^*}{\Gamma_{AR}} - \frac{\gamma_B^*}{\Gamma_{BR}}\right) \int_0^{\gamma_R^*} \exp\left(\frac{-f_B^{-1}(\hat\delta_5)}{\Gamma_{BD}} - \frac{\gamma_{RD}}{\Gamma_{RD}}\right) d\gamma_{RD}$$

$$\Im[g_2;V_6] = \frac{1}{\Gamma_{RD}\Gamma_{BR}} \exp\left(\frac{-f_A^{-1}(1)}{\Gamma_{AD}} - \frac{\gamma_A^*}{\Gamma_{AR}}\right) \int_0^{\gamma_R^*}\int_0^{\gamma_B^*} \exp\left(\frac{-f_B^{-1}(\hat\delta_6)}{\Gamma_{BD}} - \frac{\gamma_{BR}}{\Gamma_{BR}} - \frac{\gamma_{RD}}{\Gamma_{RD}}\right) d\gamma_{BR}\,d\gamma_{RD}$$

$$\Im[g_2;V_7] = \frac{1}{\Gamma_{RD}\Gamma_{AR}} \exp\left(\frac{-f_A^{-1}(1)}{\Gamma_{AD}} - \frac{\gamma_B^*}{\Gamma_{BR}}\right) \int_0^{\gamma_R^*}\int_0^{\gamma_A^*} \exp\left(\frac{-f_B^{-1}(\hat\delta_7)}{\Gamma_{BD}} - \frac{\gamma_{AR}}{\Gamma_{AR}} - \frac{\gamma_{RD}}{\Gamma_{RD}}\right) d\gamma_{AR}\,d\gamma_{RD}$$

$$\Im[g_2;V_8] = \frac{1}{\Gamma_{RD}\Gamma_{AR}\Gamma_{BR}} \exp\left(\frac{-f_A^{-1}(1)}{\Gamma_{AD}}\right) \int_0^{\gamma_R^*}\int_0^{\gamma_B^*}\int_0^{\gamma_A^*} \exp\left(\frac{-f_B^{-1}(\hat\delta_8)}{\Gamma_{BD}} - \frac{\gamma_{AR}}{\Gamma_{AR}} - \frac{\gamma_{BR}}{\Gamma_{BR}} - \frac{\gamma_{RD}}{\Gamma_{RD}}\right) d\gamma_{AR}\,d\gamma_{BR}\,d\gamma_{RD} \quad (45)$$

**Tad Matsumoto** (S'84−SM'95−F'10) received his B.S., M.S., and Ph.D. degrees from Keio University, Yokohama, Japan, in 1978, 1980, and 1991, respectively, all in electrical engineering. He joined Nippon Telegraph and Telephone Corporation (NTT) in April 1980. Since he engaged in NTT, he was involved in a lot of research and development projects, all for mobile wireless communications systems. In July 1992, he transferred to NTT DoCoMo, where he researched Code-Division Multiple-Access techniques for Mobile Communication Systems. In April 1994, he transferred to NTT America, where he served as a Senior Technical Advisor of a joint project between NTT and NEXTEL Communications. In March 1996, he returned to NTT DoCoMo, where he served as a Head of the Radio Signal Processing Laboratory until August of 2001; He worked on adaptive signal processing, multiple-input multiple-output turbo signal detection, interference cancellation, and space-time coding techniques for broadband mobile communications. In March 2002, he moved to University of Oulu, Finland, where he served as a Professor at Centre for Wireless Communications. In 2006, he served as a Visiting Professor at Ilmenau University of Technology, Ilmenau, Germany, funded by the German MER-CATOR Visiting Professorship Program. Since April 2007, he has been serving as a Professor at Japan Advanced Institute of Science and Technology (JAIST), Japan, while also keeping the position at University of Oulu. Prof.

Matsumoto has been appointed as a Finland Distinguished Professor for a period from January 2008 to December 2012, funded by the Finnish National Technology Agency (Tekes) and Finnish Academy, under which he preserves the rights to participate in and apply to European and Finnish national projects. Prof. Matsumoto is a recipient of IEEE VTS Outstanding Service Award (2001), Nokia Foundation Visiting Fellow Scholarship Award (2002), IEEE Japan Council Award for Distinguished Service to the Society (2006), IEEE Vehicular Technology Society James R. Evans Avant Garde Award (2006), and Thuringen State Research Award for Advanced Applied Science (2006), 2007 Best Paper Award of Institute of Electrical, Communication, and Information Engineers of Japan (2008), Telecom System Technology Award by the Telecommunications Advancement Foundation (2009), IEEE Communication Letters Exemplifying Reviewer Award (2011), and Nikkei Wireless Japan Award (2012). He is a Fellow of IEEE and a Member of IEICE. He is serving as an IEEE Vehicular Technology Distinguished Lecturer during the term July 2011-June 2015.